PROGRAMMABLE SILICON NITRIDE PHOTONIC INTEGRATED CIRCUITS

*Hao Tian[1], Alaina G. Attanasio[1], Anat Siddharth[2], Andrey Voloshin[2], Viacheslav Snigirev[2], Grigory Lihachev[2], Andrea Bancora[2], Vladimir Shadymov[2], Rui N. Wang[2], Johann Riemensberger[2], Tobias J. Kippenberg[2], and Sunil A. Bhave[1,]**

[1] OxideMEMS Lab, Purdue University, West Lafayette, IN, USA

[2] Laboratory of Photonics and Quantum Measurements, Swiss Federal Institute of Technology Lausanne (EPFL), Lausanne, Switzerland

ABSTRACT

Silicon Nitride (Si_3N_4) photonic integrated circuits (PICs) have emerged as core technology in a variety of applications ranging from LIDAR to quantum control and computing. However, the need for high-speed, low-voltage tuning and modulation has been a long standing challenge because Si_3N_4 lacks electro-optic effect. In this work, we demonstrate power efficient (nW) and fast (sub-μs) piezoelectric tuning of Si_3N_4 optical microring resonators by monolithically integrating Lead Zirconate Titanate (PZT) piezoMEMS actuators. We achieve, for the first time, the co-integration of PZT and thermal actuators, enabling the tuning of optical resonances over one free spectral range (FSR). The programmability is demonstrated by aligning two optical resonators fabricated on separate chips, which is the first step towards fiber-optic connected optomechanical sensors and computing networks. We further show acousto-optic modulation (AOM) of Si_3N_4 photonics using the High-overtone Bulk Acoustic Resonators (HBAR) excited by PZT actuators with modulation frequency up to 2 GHz.

KEYWORDS

Piezoelectric actuator; Si_3N_4 microring resonator; Stress-optic effect; Acousto-optic modulator.

INTRODUCTION

Integrated photonics has attracted much attention recently, because of its ability to miniaturize the optical technologies developed in research labs into commercialized products from atomic clocks [1], integrated semiconductor lasers [2], light detection and ranging (LiDAR) [3], to optical gyroscopes [4]. In the past decade Si_3N_4 photonic circuits have emerged as one key platform, due to its ultra-low optical loss from visible to mid-infrared, and large Kerr nonlinearity $\chi^{(3)}$ [5]. It has been successfully applied in the generation of dissipative Kerr soliton microcombs [6], supercontinuum generation [7], as well as photonic quantum computing circuits [8]. However, the lack of an electro-optic property has presented a major challenge to actively tune Si_3N_4 photonics, a feature that is highly desirable for feedback control, compensating fabrication errors, and programmable PICs for optical sensing and computing networks.

Conventionally, thermal-optical tuning with integrated micro-heater is employed, at the expense of speed (~ms) and power consumption (~mW) [9]. Although hybrid integration with electro-optical materials, such as lead zirconate titanate (PZT) [10], lithium niobate ($LiNbO_3$) [11], and barium titanate ($BaTiO_3$) [12], has provided an alternative way, further improvements in fabrication technology are necessary to increase the optical Q and engineer the optical dispersion for frequency comb generation.

Most recently, many efforts have been devoted to the development of stress-optic tuning of Si_3N_4 by monolithically integrating piezoelectric actuators on top of the Si_3N_4 photonics. Upon applying voltage to the actuator, it will deform due to the piezoelectric effect, which generates stress around the Si_3N_4 optical waveguide and changes its refractive index via the stress-optic effect. The change of refractive index tunes the optical response of the photonic devices. As a well-known piezoelectric material, Aluminum Nitride (AlN) actuators have been applied in tuning Si_3N_4 photonics [13]. Many promising applications have been successfully demonstrated from tunable optical frequency combs [14], semiconductor lasers [15], entangled photon pairs [16], to photonic computing networks [17]. However, the achievable tuning efficiency of an optical resonance is limited to around 20MHz/V, due to the relatively small piezoelectric coefficient of AlN. This inevitably requires a large applied voltage on the order of 100 V. While CMOS circuits can achieve such high voltages on-chip, the charge-discharge pump circuits are slow, which limits the system tuning speed.

As the traditional piezoelectric ceramic, PZT has regained much attention in tuning photonic circuits due to the maturity of depositing high quality PZT thin films on photonic chips. Many pioneering works have been done in PZT tuning of photonic circuits in both released [18] and unreleased structures [19], [20]. In this work, by integrating a disk PZT actuator on an unreleased photonic chip, we demonstrate the most efficient tuning of a Si_3N_4 microring resonator to date. Due to its much larger piezoelectric coefficient, 578 MHz/V tuning is achieved, more than one order of magnitude bigger than the AlN actuator. In addition to the PZT actuator, we also co-integrate a micro-heater on the same optical resonator, which enables a much larger tuning range. Beyond the quasi-DC tuning, we realize microwave frequency AOM by exciting HBAR modes in the substrate. This combination of PZT actuator, heater, and AOM provides a comprehensive toolset to program the PICs with more degrees of freedom, making PZT a universal platform.

DEVICE DESIGN

Figure. 1(a) shows the optical image of the fabricated disk shaped PZT actuator on top of a Si_3N_4 microring resonator, which consists of a microring and a bus

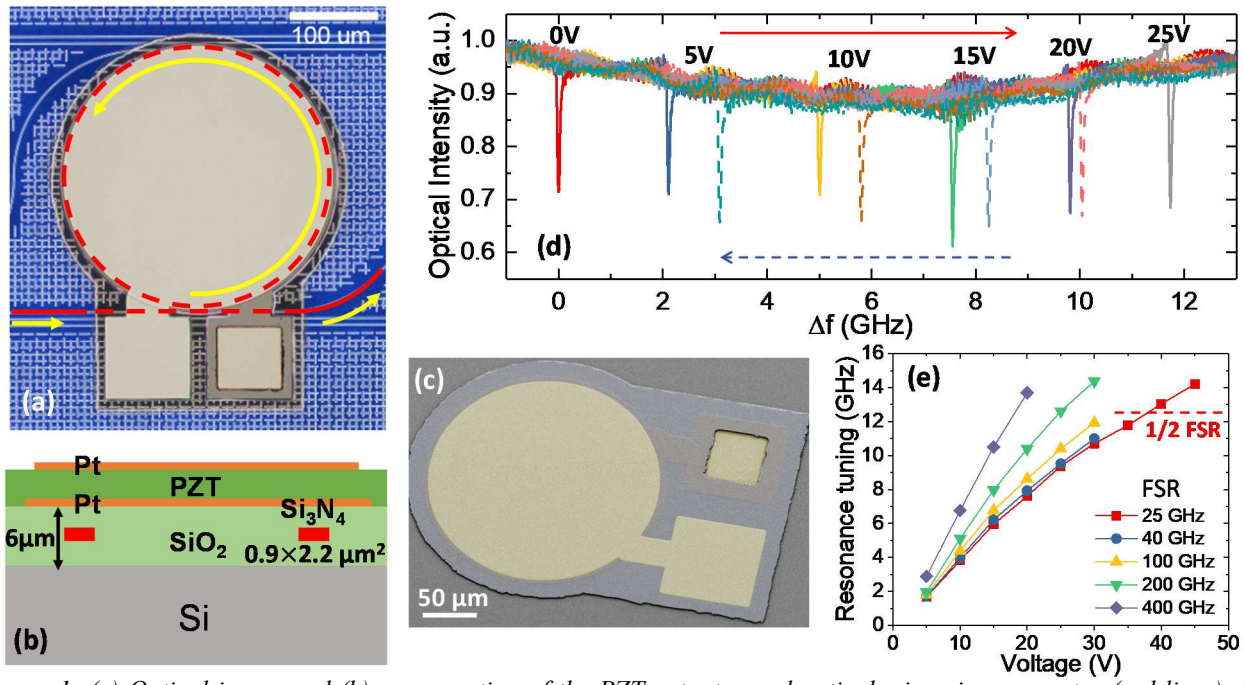

Figure 1: (a) Optical image and (b) cross-section of the PZT actuator and optical microring resonator (red lines). (c) False colored SEM of the PZT actuator. (d) Optical spectrum showing tuning of one optical resonance with increasing (solid lines) and decreasing (dashed lines) applied voltage. (d) Resonance tuning vs. Voltage for different FSR microrings.

waveguide (red lines). Light is injected and guided through the bus waveguide, which is then coupled into the microring via an evanescent field and trapped in the optical resonator at optical resonances. The resonator supports a series of equidistant optical resonances, with the spacing between them defined as the FSR, which is inversely proportional to the radius R. Devices with different radii were studied systematically. The cross-section is illustrated in Fig. 1(b). 1 μm PZT film is sandwiched between top and bottom electrodes made from 100 nm Platinum (Pt). The Si_3N_4 waveguide (0.9×2.2 μm^2) is embedded inside a 6 μm SiO_2 cladding and is 3 μm away from the bottom electrode for preserving the low loss of the optical waveguide. The whole structure sits on an unreleased high resistivity Si substrate. Optimum tuning is achieved when the waveguide is 8 μm inside the top metal. The Scanning Electron Microscopy (SEM) image of the PZT actuator is shown in Fig. 1(c), where the bottom electrode can be accessed through a via in the PZT layer.

OPTICAL RESONANCE TUNING

PZT is a ferroelectric material deposited using sol-gel technology. We apply 25 V to the actuator for at least one second to align the ferroelectric domains before device operation. We found the poling increased the tuning efficiency by a factor of two. Figure 1(d) shows the piezoelectric tuning of an optical resonance of a microring with R=115 μm (FSR=200 GHz) under different voltages. The resonance frequency is red-shifted monotonically with increasing voltages and we determine a tuning of up to 10 GHz with a voltage of less than 20V, which corresponds to a modulation efficiency of 500 MHz/V. Due to the ferroelectricity of PZT, hysteresis is observed as the voltage is gradually decreased (dashed curves). This feature can serve as an optical-readout memory element in the future. To maintain the direction of the polarization of the film, only positive voltage is applied. The application of negative voltage will reverse the polarization which tends to align with the electric field. Hence unlike AlN [13], we find that the tuning under positive and negative voltages has the same tuning direction. Thus, in real applications, an offset voltage should be applied if bi-directional tuning is required. Moreover, a high optical Q of 3 Million is maintained, which is important for tunable frequency comb and frequency-agile laser. The leakage current is kept below 1 nA at 20 V due to the high quality of PZT film. This enables ultra-low static power consumption on the order of tens of nano-Watts. The power efficiency, defined as the power consumption per tuning frequency, is 2 pW/MHz.

The tuning of microring resonators with different radii (and FSRs) is studied in Fig. 1(e). Small radius rings have larger FSR. It can be found that the tuning efficiency increases as the device size decreases (FSR increases), since the relative change of radius $\Delta r/r$ increases as the ring deforms which contributes to the relative change of resonance frequency $\Delta f/f_0$, besides the stress-optic effect. All the devices achieve tuning bigger than 10 GHz when the voltage is larger than 30 V. However, as the voltage further increases, the tuning tends to saturate due to the saturation of the polarization of PZT at high electric fields. This leads to a nonlinear response for large signals, which can be compensated with a pre-conditioned input signal.

Interestingly, for the 25 GHz FSR device, tuning over half FSR is achieved under 40 V, corresponding to a π phase shift of light. This can be understood that, with 2π phase shift, light will shift from one resonance to the next harmonic, which is one FSR. We calculate the figure of merit (modulation length product) $V_\pi \cdot L = 22$ V·cm, where V_π is the voltage that produces π phase shift of the light. Although this value is an order of magnitude larger than that for the state of the art electro-optic tuning using

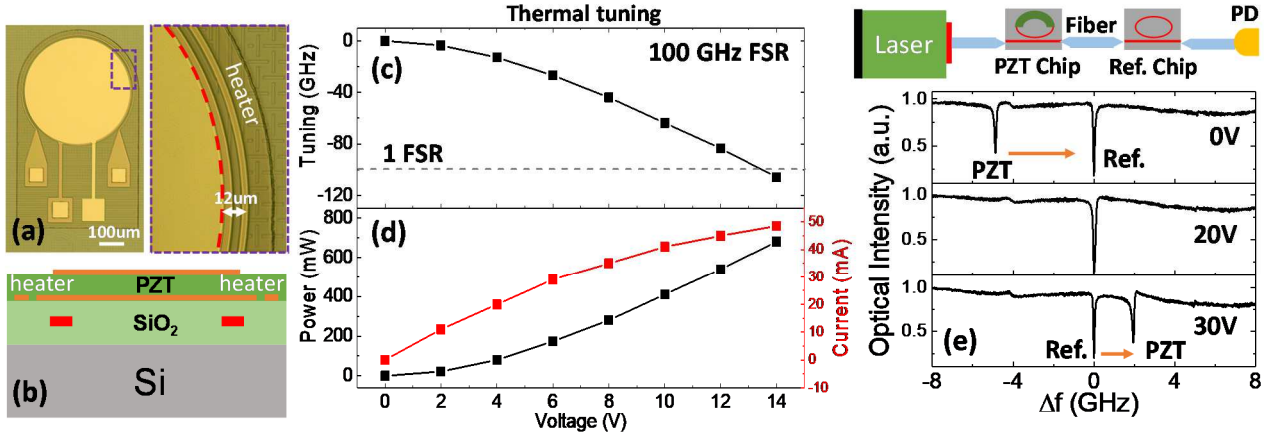

Figure 2: (a) Optical image and (b) cross-section of PZT actuator co-integrated with heater. (c) Resonance tuning via heater under different voltages, and correspondingly (d) power consumption (left Y-axis) and current (right Y-axis). (e) Demonstration of aligning one resonance to a reference (Ref.) optical resonator on a separate chip using solely PZT actuator. The resonances become aligned under 20 V with initial misalignment of 5 GHz. PD: Photodetector.

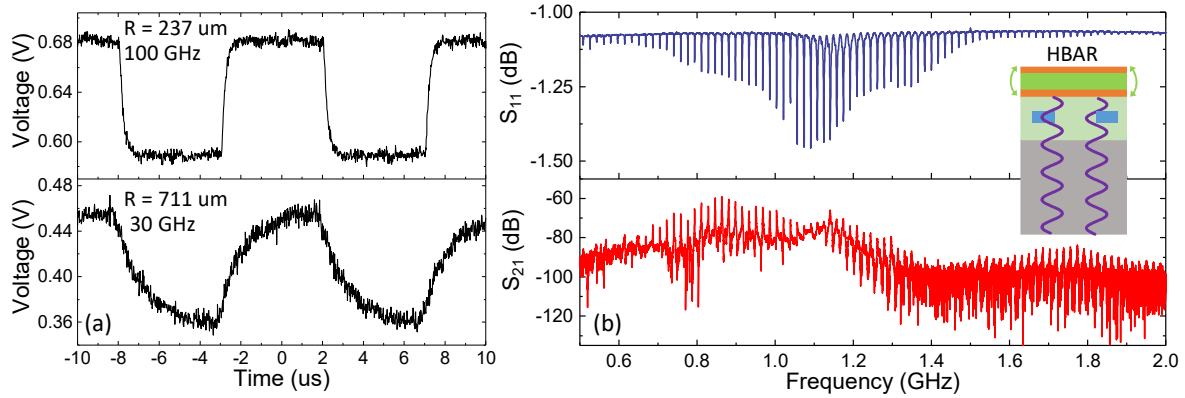

Figure 3: (a) Dynamic response under 100kHz square wave signals(V_{pp}=1V) for 100GHz FSR (upper, R=237μm) and 30GHz FSR (lower, R=711μm) devices. The laser is biased at the slope of the optical resonance, and Y-axis is the voltage output from the photodetector. (b)Electromechanical S_{11}(upper) and Optomechanical (S_{21}) responses, showing periodic (spacing of 17.6MHz) HBAR modes and efficient AOM. Inset: schematic of HBAR mode formed in the substrate.

$LiNbO_3$ [21], the modulation loss product $V_\pi \cdot L \cdot \alpha$ = 1.87 V·dB is comparable to 1 V·dB of $LiNbO_3$, thanks to the ultra-low loss of the Si_3N_4 waveguide (0.085 dB/cm).

CO-INTEGRATION WITH HEATER

We further demonstrate the compatibility of piezo-electric and thermal tuning by incorporating micro-heaters into the bottom metal layer at no cost for extra masks (Fig. 2(a), (b)). However, to have efficient thermal tuning, the optical ring has to be brought close to the micro-heater such that the ring is congruent with the top metal edge. This reduces the overlap of the optical mode and stress field and lowers the stress-optic tuning by half. Thermal tuning of a device with 100 GHz FSR (R=237 μm) is shown in Fig. 2(c) where over one full FSR is achieved under 14 V, at the expense of 700 mW (Fig. 2(d)). This shows the ability of coarse tuning (long range) via heater along with fine tuning (fast speed) with piezoelectric actuators (see Fig. 2(e)).

To demonstrate programmability, the resonances of optical resonators fabricated on two separate chips are aligned through the PZT actuator (Fig. 2(e)). Initially at 0V, the spacing between them is 5 GHz. By applying 20V at the PZT actuator, there is only one resonance in the transmission spectrum showing good alignment. As we further increase the voltage, the resonance of the PZT chip crosses over the reference chip. This demonstrates the ability to compensate resonance misalignment induced by the fabrication variation, which is required to build scalable PIC multi-chip modules (MCMs).

ACOUSTO-OPTIC MODULATION

The tuning speed is characterized by applying a 100 kHz square wave voltage to the PZT, while measuring the transmitted light intensity by biasing the laser at the slope of the optical resonance, as shown in Fig. 3(a). For a small device with R=237 μm, the PZT actuator achieves switching between two states, with the response time limited to 0.2 μs by the capacitive time constant due to the large permittivity of PZT. It becomes more obvious for a large device with R=711 μm, where it takes 1.4 μs to respond.

Beyond this quasi-DC tuning, HBAR modes can be excited at microwave frequencies through the PZT actuator, where bulk acoustic waves are confined in the acoustic Fabry-Pérot cavity formed by the top and bottom surfaces of the photonic chip. A series of mechanical resonances is formed up to 2 GHz, which are distributed evenly with spacing of 17.6 MHz (see Fig. 3(b)). Efficient acousto-optic modulation is achieved between 0.8-1 GHz. This high frequency AOM will add more functionalities to

Table 1: Comparison with state of the art piezoelectric tuning of Si_3N_4 microring resonators.

Ref.	Material	Structure	FSR (GHz)	Radius (µm)	Optical Q	Tuning (MHz/V)	Speed (µs)	Power (pW/MHz)	$V_\pi \cdot L$ (V·cm)
[13]	AlN	Unreleased	200	118	6.5M	25	0.05	20	124
[18]	PZT	Released	52	580	0.086M	3250	3.7	3	3.6
[19]	PZT	Unreleased	48	625	3.6M	200	NA	5	43
PZT w/o heater	PZT	Unreleased	400	57	3.56M	578	0.1	1.7	18
PZT w/ heater	PZT	Unreleased	100	237	2.2M	243	0.2	4	30

the platform, such as the generation of Pound-Drever-Hall error signal for locking the optical resonance to an external laser source [19].

In conclusion, we demonstrate a programmable Si_3N_4 photonic circuit that is capable of low power, fast tuning through PZT piezoMEMS actuators, and large range tuning via micro-heaters. From the comparison in Table 1, it can be seen our PZT actuator possesses both large tuning efficiency, sub-µs speed, and the highest power efficiency. Therefore, our PZT-on-SiN Photonics platform lays the foundation for Si_3N_4 PICs for sensing and communication networks.

ACKNOWLEDGEMENTS

The authors would like to thank DARPA MTO under contract No. W911NF2120248 (NINJA LASER); European Union's H2020 research and innovation program; FET Proactive Grant No. 732894 (HOT); NSF QISE-NET DMR 17-47426; SNSF Ambizione Fellowship (201923);ESA Contract No. 4000135357/21/NL/GLC/my. Photonic chips were fabricated in the EPFL Center of MicroNano-Technology (CMi), and PZT actuators were fabricated by Radiant Technologies Inc.

REFERENCES

[1] Z. L. Newman *et al.*, "Architecture for the photonic integration of an optical atomic clock," *Optica*, vol. 6, no. 5, pp. 680–685, 2019.

[2] W. Jin *et al.*, "Hertz-linewidth semiconductor lasers using CMOS-ready ultra-high-Q microresonators," *Nat. Photonics*, pp. 1–8, 2021.

[3] P. Trocha *et al.*, "Ultrafast optical ranging using microresonator soliton frequency combs," *Science (80-.).*, vol. 359, no. 6378, pp. 887–891, 2018.

[4] S. Gundavarapu *et al.*, "Interferometric Optical Gyroscope Based on an Integrated Si_3N_4 Low-Loss Waveguide Coil," *J. Light. Technol.*, vol. 36, no. 4, pp. 1185–1191, 2018.

[5] D. J. Moss, R. Morandotti, A. L. Gaeta, and Lipson Michal, "New CMOS-compatible platforms based on silicon nitride and Hydex for nonlinear optics," *Nat. Photonics*, vol. 7, no. 8, pp. 597–607, 2013.

[6] T. J. Kippenberg, R. Holzwarth, and S. A. Diddams, "Microresonator-based optical frequency combs.," *Science*, vol. 332, no. 6029, pp. 555–9, 2011.

[7] A. L. Gaeta, M. Lipson, and T. J. Kippenberg, "Photonic-chip-based frequency combs," *Nat. Photonics*, vol. 13, no. 3, pp. 158–169, 2019.

[8] J. M. Arrazola *et al.*, "Quantum circuits with many photons on a programmable nanophotonic chip," *Nature*, vol. 591, no. 7848, pp. 54–60, 2021.

[9] X. Xue *et al.*, "Thermal tuning of Kerr frequency combs in silicon nitride microring resonators," *Opt. Express*, vol. 24, no. 1, p. 687, 2016.

[10] K. Alexander *et al.*, "Nanophotonic Pockels modulators on a silicon nitride platform," *Nat. Commun.*, vol. 9, no. 1, p. 3444, 2018.

[11] A. N. R. Ahmed, S. Shi, M. Zablocki, P. Yao, and D. W. Prather, "Tunable hybrid silicon nitride and thin-film lithium niobate electro-optic microresonator," *Opt. Lett.*, vol. 44, no. 3, pp. 618–621, 2019.

[12] S. Abel *et al.*, "Large Pockels effect in micro- and nanostructured barium titanate integrated on silicon," *Nat. Mater.*, vol. 18, no. 1, pp. 42–47, 2019.

[13] H. Tian *et al.*, "Hybrid integrated photonics using bulk acoustic resonators," *Nat. Commun.*, vol. 11, 3073, 2020.

[14] J. Liu *et al.*, "Monolithic piezoelectric control of soliton microcombs," *Nature*, vol. 583, no. 7816, pp. 385–390, 2020.

[15] G. Lihachev *et al.*, "Low-noise frequency-agile photonic integrated lasers for coherent ranging," *Nat. Commun.*, vol. 13, 3522, 2022.

[16] T. Brydges *et al.*, "An Integrated Photon-Pair Source with Monolithic Piezoelectric Frequency Tunability," *arXiv Prepr. arXiv2210.16387*, pp. 1–9, 2022.

[17] M. Dong *et al.*, "High-speed programmable photonic circuits in a cryogenically compatible, visible–near-infrared 200 mm CMOS architecture," *Nat. Photonics*, vol. 16, no. 1, pp. 59–65, 2022.

[18] W. Jin, R. G. Polcawich, P. A. Morton, and J. E. Bowers, "Piezoelectrically tuned silicon nitride ring resonator," *Opt. Express*, vol. 26, no. 3, pp. 3174–3187, 2018.

[19] J. Wang, K. Liu, M. W. Harrington, R. Q. Rudy, and D. J. Blumenthal, "Silicon nitride stress-optic microresonator modulator for optical control applications," *Opt. Express*, vol. 30, no. 18, p. 31816, 2022.

[20] N. Hosseini *et al.*, "Stress-optic modulator in TriPleX platform using a piezoelectric lead zirconate titanate (PZT) thin film," *Opt. Express*, vol. 23, no. 11, pp. 14018–14026, 2015.

[21] C. Wang *et al.*, "Integrated lithium niobate electro-optic modulators operating at CMOS-compatible voltages," *Nature*, vol. 562, no. 7725, pp. 101–104, 2018.

CONTACT

*Sunil A. Bhave, mobile: +1-510-390-3269;
bhave@purdue.edu